The structure and properties of horse muscle acylphosphatase in solution

Mobility of antigenic and active site regions

Vladimir Saudek, Robert J.P. Williams and Giampietro Ramponi°

Inorganic Chemistry Laboratory, University of Oxford, South Parks Road, Oxford OX1 3QR, England and °*Department of Biological Sciences, University of Florence, Florence, Italy*

The solution structure of acylphosphatase determined by proton nuclear magnetic resonance spectroscopy is described. The results allow us to discuss the fold of the protein (101 amino acids), to correlate the exposure and the mobility of the backbone with the antigenicity, and to locate the active site.

1. INTRODUCTION

In this paper we provide for the first time the structure of an enzyme in solution. It was achieved without the assistance of any crystallographic data. The method of study, high resolution nuclear magnetic resonance (NMR), allows a discussion not only of the structure but also the mobility of the backbone, the active site and the antigenic regions.

Acylphosphatase is a vertebrate enzyme (EC 3.6.1.7) catalysing the hydrolysis of organic acylphosphates [1]. Its highly conserved sequence is a single chain with its most variable part at the N-terminus [2]. It is isolated by us as a mixed disulphide with glutathione [3]. Neither the variable N-terminus nor the glutathione are important for activity. No X-ray diffraction analysis of it has been performed because of the lack of suitable crystals.

Correspondence address: R.J.P. Williams, Inorganic Chemistry Laboratory, University of Oxford, South Parks Road, Oxford OX1 3QR, England

2. MATERIALS AND METHODS

The enzyme was isolated as described [3]. It was dissolved in 0.05 mol/l deuteroacetic acid in ^2H_2O or H_2O to give a concentration $4–6 \times 10^{-3}$ mol/l. The pH of the solution was 3.2. The NMR structural study was performed using standard NMR techniques [4] described in detail [5,6]. The data were collected at 500 MHz using either a Bruker AM500 or a home-built spectrometer [6]. A set of well resolved two dimensional spectra was obtained (correlated, relayed coherence correlated and nuclear Overhauser enhancement (NOE)) of the sample in ^2H_2O as well as in H_2O. NOE build-up [4] was followed using mixing times of 80, 100, 150, 200, 300 and 350 ms and any spin diffusion effects were eliminated.

3. RESULTS AND DISCUSSION

Sequence specific assignment of the resonances (table 1) will be described in detail elsewhere since it is not possible to provide such data in a short paper. Representative examples of the NMR spectra can be seen in our previous papers [5,6]. The NOE spectra carried out at different mixing times make it possible to produce a list of NMR constraints: NOE spectra are now well understood and the NOE detected can be translated into upper limits of distances between hydrogens in the

Table 1

Chemical shift in the assigned ¹H NMRs of horse muscle acylphosphatase

Amino acid	Chemical shift (ppm)[a]			Others
	HN	HA	HB	
2 T	7.80	4.33	4.42	HG 1.26
3 A	8.18	4.37	1.42	
4 R	8.23	4.65	1.83 1.99	HD 3.11 HG HE 7.42
5 P	–	4.49	2.33 2.03	HD 3.72 3.78 HG 2.07
6 L	8.47	4.65	2.18	HG 1.85 HD 0.71 0.72
7 K	8.78	5.40	1.63 1.74	
8 S	8.62	5.69	3.67	
9 V	9.11	4.56	2.10	HD 0.87 1.26
10 D	8.74	5.47	2.66 3.65	
11 Y	7.92	5.96	2.35 2.53	HD 6.70 HE 6.43
12 F	8.29	5.01	1.80 2.00	HG 1.47
13 V	9.50	4.56	1.71	HG 0.97 1.07
14 F	8.92	5.12	3.03 3.06	HD 7.18 HE+HZ 7.15
15 G	(8.28	3.96) (4.07)		
16 R	9.34	4.10	2.07 2.32	HD 3.25 HE 7.26[c]
17 V	7.04	4.06	1.60	HG 0.84 0.90
18 Q	8.11	4.42	1.80 1.99	HG 2.35
19 G		4.80 4.85		
20 V	7.61	4.28	1.75	HG 0.31 0.58
21 C	9.05	4.51	3.95	
22 F	(8.30)	3.97	3.03 3.52	HD 7.13 HE 7.20 HZ 7.17
23 R	8.70	4.10	2.23 2.43	HG 2.34 HE 7.58 HD 3.00 3.42
24 M	7.50	4.17	2.17 2.26	HG 2.69
25 Y	8.07	4.10	3.02 3.08	HD 7.57 HE 6.78
26 A	8.77	3.00	1.32	
27 E	7.78	3.74	2.17 2.26	HG 2.41 2.56
28 D	7.62	4.22	2.54 2.60	
29 E	7.79	3.69	0.99 0.48	HG 1.43
30 A	7.87	3.47	0.24	
31 R	7.64	4.19	1.93	HG 1.76 HD 3.28 HE 7.14
32 K	7.55	3.93	1.50 1.81	HG 1.45 HD 1.26
33 I	8.07	3.97	1.74	HG1 1.45 1.17 HG2 0.90 HD 0.71
34 G	8.12	3.85 4.25		
35 V	7.46	4.93	2.44	HG 0.67 0.68
36 V	8.67	4.74	2.25	HG 0.75 1.12
37 G	8.39	2.42 5.20		
38 W	8.15	5.00	2.38 3.03	HNZ 6.98 HZ2 7.31 HE3 6.97 HZ3 6.73 HD1 6.14 HE1 10.40 HG 1.30 1.40
39 V	8.05	5.17	2.25	
40 K	9.30	4.82	1.92 2.00	

Table 1 (contd.)

Chemical shift in the assigned ¹H NMRs of horse muscle acylphosphatase

Amino acid	Chemical shift (ppm)[a]			Others
	HN	HA	HB	
41 N	9.10	5.31	2.83 2.88	HG 6.97 7.53
42 T	8.37	4.78	4.62	HG 1.12
43 S	(8.37	4.50	3.97 4.06)	
44 K	7.47	4.57	1.74 2.01	(HG 1.45)
45 G	7.74	3.65 4.27		
46 T	6.84	4.71	0.94	HG 0.50
47 V	7.90	5.12	1.53	HG 0.78 1.09
48 T	9.23	5.10	3.74	HG 1.03
49 G	6.33	0.94 3.26		
50 Q	5.93	5.30	1.62 1.7	HG 2.36 HD 6.97 8.83
51 V	9.19	5.27	2.04	HG 1.08 1.09
52 Q	9.18	6.00	2.10 2.35	HG 2.75 HD 6.98 7.20
53 G	8.33	4.41 4.02		
54 P	–	4.75	1.90 2.63	HD 3.45 3.92 HG 2.13
55 E	8.67	3.50	2.03 2.17	HG 1.45
56 E	9.73	4.04	2.08 2.17	HG 2.45
57 K	7.11	4.08	1.60 1.80	HG (1.42)
58 V	8.08	3.20	1.84	HG 5.98 6.06
59 N	8.35	4.25	2.82 2.87	HD 6.76 7.55
60 S	7.72	4.33	3.93 4.05	
61 M	8.09	4.36	2.20 2.37	HG 2.1
62 K	8.94	3.80	1.51 1.78	HG 0.42 HD 1.20
63 S	7.76	4.16	3.95 4.0	
64 W	7.93	3.95	3.20 3.55	HE1 10.19 HD 6.83 HE 7.19 HZ3 6.48 HH 6.18 HZ2 8.64
65 L	8.51	3.91	1.38 2.16	HG 2.04 HD 0.04 0.95
66 S	7.64	4.65	4.12	
67 K	7.91	4.27	1.96 2.11	HD 2.20 HG 1.55
68 V	7.52	3.89	1.03	HG 0.76 0.85
69 G	7.74	3.97 3.53		
70 S	8.51	4.99	3.57 3.80	
71 P	–	4.23	1.87 2.26	HG 1.99 2.90 HD 3.43 3.91
72 S	7.83	4.50	3.94 3.97	
73 S	8.49	4.89	3.23 3.31	HD 3.25 HE 6.99[c]
74 R	8.22	8.85	2.58	HD 0.43 HG2 0.78 HG1 0.60 0.78
75 I	8.78	3.80	1.44	
76 D	9.35	4.75	2.38 2.68	HG 1.33 HD 2.86 HE 8.62
77 R	7.63	4.50	0.76 1.78	
78 T	8.29	5.13	4.11	HG 4.07

Table 1 (contd.)

Chemical shift in the assigned ^{1}H NMRs of horse muscle acylphosphatase

Amino acid	Chemical shift (ppm)[a]			
	HN	HA	HB	Others
79 N	9.18	5.00	2.77 2.90	HG 6.67 7.75
80 F	8.86	5.85	2.93 3.15	HD 4.72 HE 4.10 HZ 4.70
81 S	9.08	4.85	3.87	
82 N	9.00	4.14	2.73 3.00	HG 6.82 7.67
83 E	8.34	5.36	1.94 2.10	HG 2.20
84 K	9.10	4.93	1.82 1.92	HD 1.53 HG 1.25 (HZ 7.20)
85 T	8.46	4.94	4.09	HG 2.34
86 I	7.88	4.84	2.03	HG1 0.57 1.09 HG2 0.93 HD 0.83
87 S	8.77	4.45	3.85 3.87	
88 K	7.20	4.40	1.70 1.75	(HG 0.81 HD 0.99)
89 L	8.56	4.26	1.66	HG 1.89 HD 1.07 1.89
90 E	9.14	4.12	1.65 1.70	HG 1.93
91 Y	7.06	4.89	2.54 3.79	HD 7.07 HE 8.62
92 S	8.04	4.84	3.00 3.10	
93 N	9.03	4.84	1.73 1.97	
94 F	9.01	5.21	2.85 3.14	HD 6.65 HE 6.90 HZ 6.84
95 S	7.88	5.50	3.82 3.99	
96 V	8.14	4.41	1.89	HG 0.58 0.92
97 R	8.67	4.55	1.50 1.82	HG 1.48 HD 2.22 2.67 HE 5.88 6.47
98 Y	8.07	4.34	2.70 3.22	HD 6.85 HE 7.13
Glutathione (attached to C 21)				
1 E	8.27	4.55	1.76	HG 1.20 HD 3.17 3.22
2 S	(9.04	4.68	3.94 4.00)	
3 G	(8.16	4.01) (4.19)		

[a] 6×10^{-3} mol/l solutions of the protein in 0.05 mol/l acetic acid in H_2O (pH 3.2) at 37°C, referred to 2,2-trimethyl 2-silapentane-5-sulphonate with the average error ± 0.02 ppm. The values in parentheses are uncertain
[b] Assignments may be interchanged

molecule [4]. This is graphically summarised in fig.1. The diagonal shows the intraresidue NOEs. Sequential NOEs between residues i and $i + 1$ appear as squares adjacent to the diagonal and illustrate the quality of the assignment. The NOEs between residues i, $i + j$ ($j = 2,3,4$) are detected mainly for helical regions (residues number 22–34 and 55–66). The β-sheet residues (7–14, 35–42, 45–53 and 78–86) give rise to NOEs arranged in

continuous lines perpendicular to the diagonal. Fig.1 also shows that many NOEs are due to the spatial proximity of sequentially very distant parts of the molecule. Often, more than two sequentially distant parts are brought together by the fold. In summary a total of 1058 structurally meaningful distances were derived from the NOEs: 448 intra-residue, 212 short distance (between ith and up to $i + 4$th residues) and 398 long distance. (As no stereospecific assignment was made, NOEs of two protons magnetically nonequivalent for their stereochemical configuration provide information on one distance only.) Further distance constraints could be derived from H bonds detected in α-helices (19) and β-structures (22) as described previously [5,6]. The backbone torsion angle Φ, as inferred from coupling constants [4], was restricted to $-90°$ to $40°$ for 21 residues in helices, and to $-80°$ to $-160°$ for 38 residues in the β-sheet.

The three dimensional structure was determined using the distance geometry algorithm with the program DISSMAN [7]. Full description of the calculation will be described later. The calculation cannot provide a single structure which completely meets the experimental constraints. Instead, a set of structures is obtained, all of which obey the input restraints to a large extent and retain some residual violations of the experimental distances. Fifteen structures were generated for acylphosphatase. They all showed the same global fold but differed in some local conformations.

Fig.2 shows the five structures with the lowest sum of residual violations (about 10 violations of 0.11 nm, average of 0.02 nm per experimental distance for the whole molecule and 10 violations of 0.05 nm for the backbone and about 0.01 nm per distance). They are superimposed to give minimal root-mean-square deviations between each other (about 0.15 nm for the main chain and 0.2 nm for all atoms). The differences and similarities reveal how the conformation may be defined from the NMR point of view. The structures nearly coincide in the segments of the regular secondary structure. The greatest variability is observed at the N-terminus. Considering that no constraints for residues in the two loose loops connecting the β-structure and the helices (15–21 and 54–67) and the β-hairpin (43–45) were used (cf. fig.1), they appear surprisingly well defined,
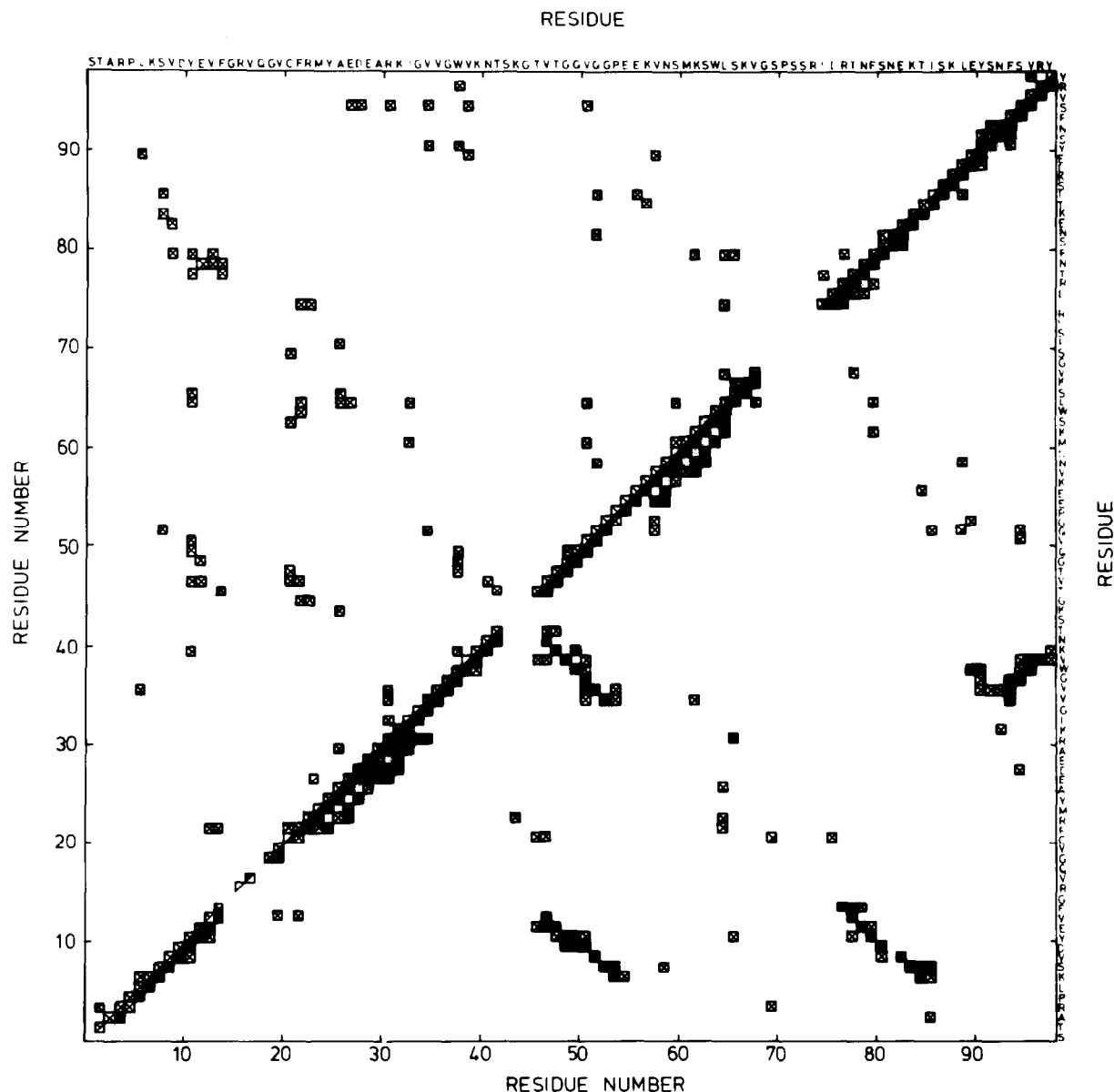
Fig.1. Plot of the NOEs observed for acylphosphatase. A square connects the residues between which a NOE was observed. The NOEs involving the backbone resonances are shown under the diagonal (■, backbone/backbone; ⊠, backbone/side chain), those involving side chains only appear over the diagonal. (For the diagonal, triangles are used.)

though not to the same degree as the rest of the structure. This is probably a consequence of the rigidity of the adjacent structures. Although the glutathione moiety (not shown in fig.2) was assigned, no NOE to the rest of the molecule was observed, indicating that glutathione is freely moving on the surface.

The β-structure contains four antiparallel strands. Two of them, 35–42 and 45–53, are connected by a tight turn to a β-hairpin at one end and via the two helices to the β-strands 7–14 and 77–86. The latter continues by a well defined chain, running on the enzyme's surface at the edge of the β-sheet, to finish in a short segment of a
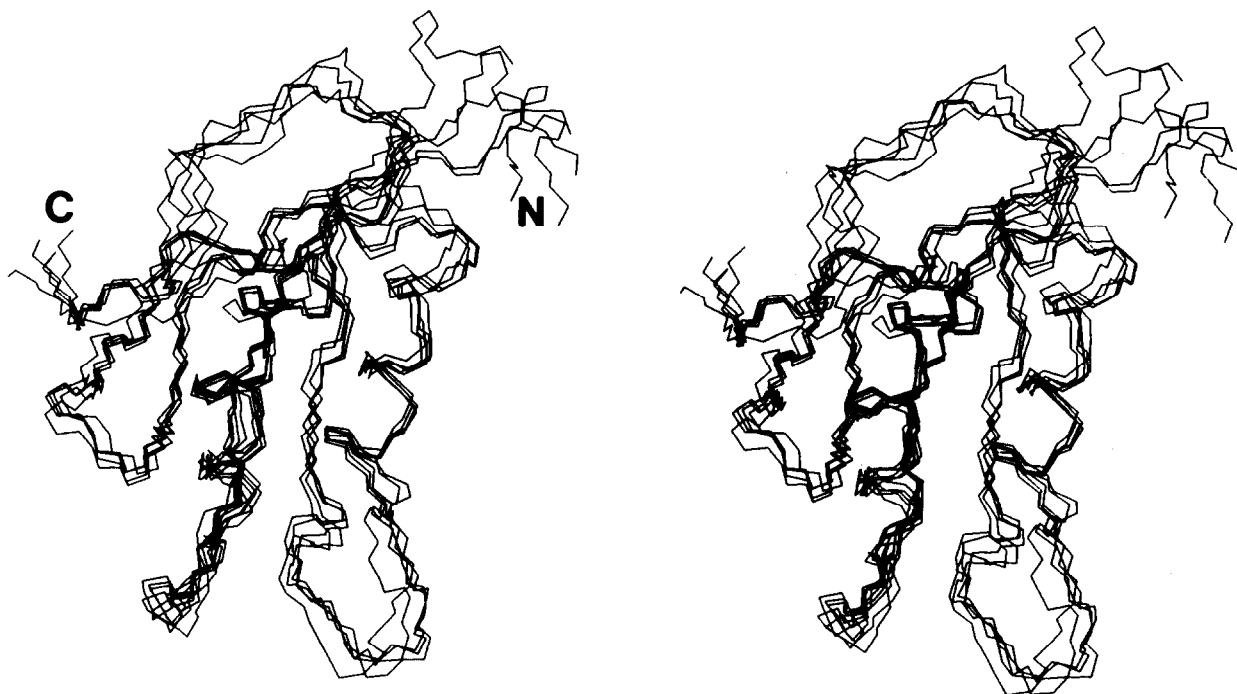
Fig.2. Stereo view of five distance geometry structures overlaid to give the minimal root-mean-square deviations between the atoms. Only backbone heavy atoms are shown.

parallel β-strand (94–98). The helices are in contact and run antiparallel. There is a β-bulge in the sheet at residue 82.

Both the β-sheet and the helices are amphiphilic. The β-sheet provides one side of the enzyme structure, while the helices form the other side; they are stuck together by a hydrophobic core built from the side chains coming from both. The hydrophilic side chains point into the solvent. In order to illustrate the heart of the hydrophobic core, all atoms within 1 nm of Leu 65 are plotted for all five structures in fig.3. Residues from both helices as well as from the β-sheet can be found in this range, and some of them even lie within the limits of NOE detection (i.e. <0.4 nm, cf. fig.1). The definition of the internal structure is remarkably clear, yet all aromatic residues flip rapidly i.e. $>10^4$ per s.

Acylphosphatase is obviously an α/β protein [8]. However, its fold differs from that of most known proteins. The secondary structure units packed together do not follow each other sequentially in the primary structure (except for the β-hairpin). Two parallel β-strands connected by a helix are not neighbours in the β-sheet as is

generally found [8]. Instead, they are separated by another antiparallel strand, consequently the resulting β-sheet is antiparallel. The whole fold can be regarded as two interleaved $\beta\alpha\beta$ packing units. A similar fold has been found in a ferredoxin which, being a sulphur-metalloprotein, has been taken as an exception and therefore difficult to classify [8].

In addition to the extensive hydrogen bonding between the peptide amides and carbonyls inside the helices and between the strands of the β-sheet, many further hydrogen bonds are indicated by the spatial proximity of hydrogen donor and acceptor groups of side chains. Some of these can be inferred from their resistance to deuterium/hydrogen exchange (e.g. Asn 79/Glu 12), but the majority, being located on the surface, escape direct detection. It seems likely, however, that there is a layer of side chains, interconnected by hydrogen bonds, on the hydrophilic face of the β-sheet. It would be this layer which ensures the observed remarkable resistance of many peptide amides in the main chain to the hydrogen/deuterium exchange.

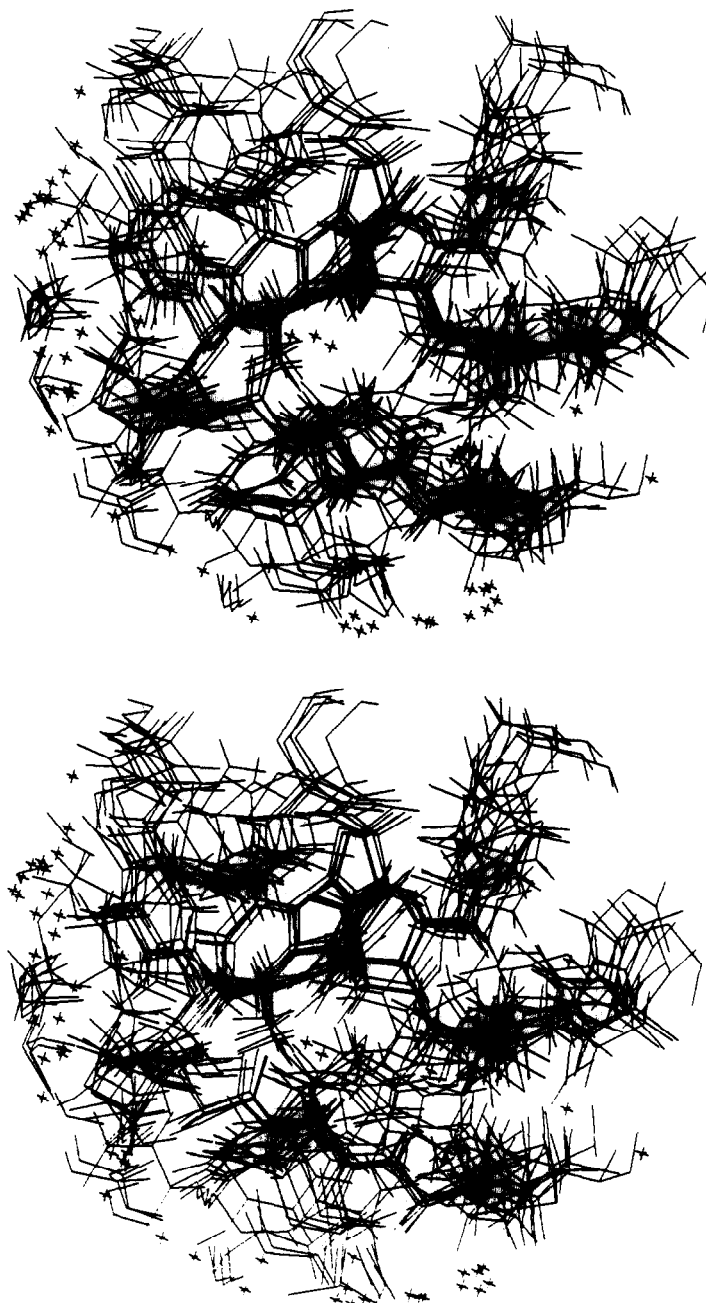Surface regions are of considerable interest

Fig.3. Stereo view of part of the hydrophobic core. All atoms within 1 nm from CA of Leu 65 are plotted for five distance geometry structures.

because they must generate both the active site and provide the observed antigenic determinants. These two types of zones are usually not identical since the first is frequently a rather rigid concave cleft while the second is thought to be a more mobile convex structure. We are able to comment on both these aspects.
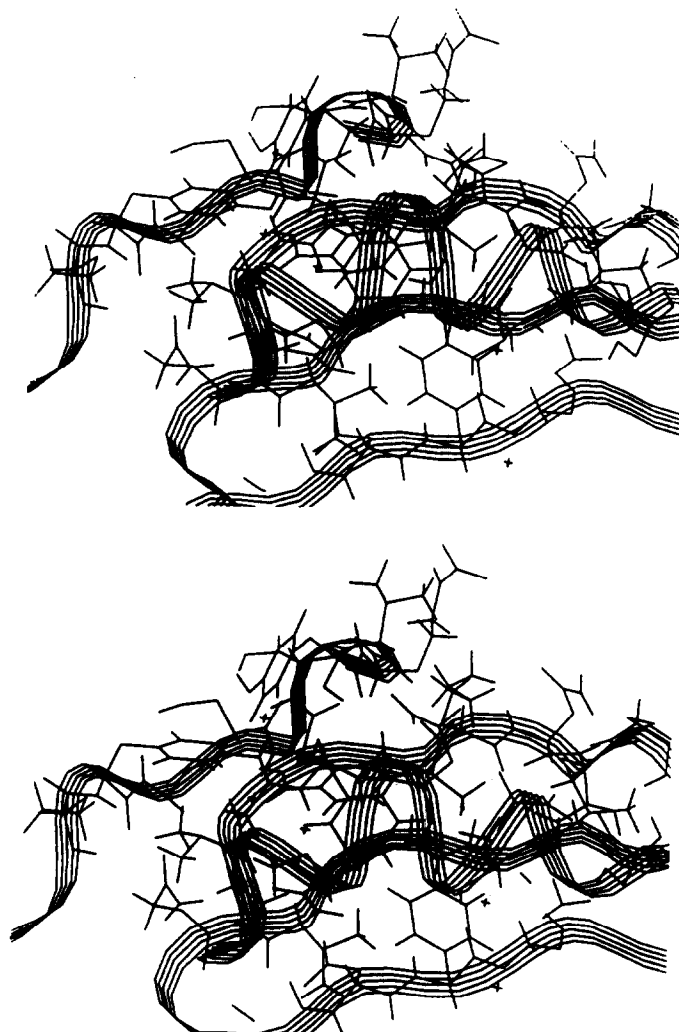
Three principal antigenic regions of acyl-

Fig.4. Stereo view of the region indicated by $[Cr(CN)_6]^{3-}$ as the active site. The main chain is emphasised by a ribbon, all atoms within 1.0 nm from CA of Tyr 98 are plotted.

phosphatase were found within segments 1–7, 45–56 and 66–80 before there was any structural knowledge [9]. Two of them contain genetically variable residues. Inspection of fig.2 reveals that these sequences encompass apparently well defined areas of structure within loops. Fig.1 shows, however, that they display much lower number of NOEs, both intra- and interresidual, than the parts within the regular secondary structure. The lack of short range NOEs indicates increased mobility (longer relaxation times and/or several possible conformations within one region) as compared to

the rest of the molecule. A striking observation is that in the longer loops and even in the tight loops 42–46 and 51–55 the NHs exchange with the solvent relatively rapidly unlike those within the rigid secondary structure of the sheet and the helices. This shows that the turns deform with much greater ease than the elements of the adjacent secondary structure. The same argument holds for the N-terminus. Fig.3 also shows that the antigenic regions are exposed on the surface of the enzyme. These findings fit the theories which suggest that the sequential antigenic regions of the proteins are

mobile segments [10] on the surface and usually form loops [11]. We note that there is another highly mobile fragment 15–21 with attached glutathione covering the loop. There is a suggestion [12] that this region is antigenic in the absence of glutathione. The two remaining loops, 33–35 and 51–55, are buried inside the protein. It is striking that the most obvious antigenic sites are the exposed loops, all of which are more mobile than the other elements.

The active site of acylphosphatase was located using experiments with $[Cr(CN)_6]^{3-}$. As this compound competitively inhibits the activity of the enzyme and is displaced by an excess of the inhibitory product phosphate, it must bind at the active site. It is an NMR relaxation probe which broadens resonances in its proximity. The experiments indicate that the active site includes the C-terminus, Tyr 98. Fig.4 shows the arrangement of the side chains in this region. They are relatively well defined. It is known from biochemical studies that side chains of at least one lysine, one other basic residue and one acidic residue are involved in the activity. The figure shows that all these functional groups can be found in the revealed region. The C-terminal tyrosine side chain itself is extremely mobile and would appear to have motion independent of the whole protein. A more precise description of the active site requires further experimental work.

REFERENCES

[1] Ramponi, G. (1975) in: Methods in Enzymology (Wood, W.A. eds) pp.409–426, Academic Press, New York.

[2] Stefani, M., Modesti, A., Camici, G., Manao, G., Cappugi, G., Berti, A. and Ramponi, G.J. (1986) Protein Chem. 5, 307–321.

[3] Manao, G., Camici, G., Stefani, M., Berti, A., Cappugi, G., Liguri, G., Nasi, P. and Ramponi, G. (1983) Arch. Biochem. Biophys. 226, 414–424.

[4] Wüthrich, K. (1986) NMR of Proteins and Nucleic Acids, John Wiley and Sons, New York.

[5] Saudek, V., Williams, R.J.P. and Ramponi, G. (1988) J. Mol. Biol. 199, 233–237.

[6] Saudek, V., Atkinson, R.A., Williams, R.J.P. and Ramponi, G. (1988) J. Mol. Biol., submitted.

[7] Braun, W. and Go, N. (1985) J. Mol. Biol. 186, 611–626.

[8] Richardson, J.S. (1981) Adv. Protein Chem. 34, 167–339.

[9] Stefani, M., Degl'Innocenti, D., Berti, A., Marzocchini, G., Camici, G., Manao, G. and Ramponi, G. (1987) J. Protein Chem. 6, 479–488.

[10] Moore, G.R. and Williams, R.J.P. (1980) Eur. J. Biochem. 103, 543–550.

[11] Dyson, H.J., Lerner, R.A. and Wright, P.E. (1988) Annu. Rev. Biophys. Biophys. Chem. 17, 305–324.

[12] Kazaki, T., Mizuno, Y., Takasawa, T. and Shiokawa, H. (1985) J. Biochem. 97, 1144–1154.